ISSN: 2414-1895 DOI: 10.6919/ICJE.202105_7(5).0002

Synchronous State of Non-parallel Shaft Unbalanced Rotors in a Three-dimensional Space and Far-resonance System

Pan Fang, Yang Li[a]

School of Mechanical Engineering, Southwest Petroleum University, Chengdu, 610000, China.

[a]Liyanger6@163.com

Abstract

The influence of the dynamic characteristics of the system on vibrating screen is the extremely important in oil drilling industry. However, synchronous behavior of the motors is the essential factor that determine the dynamic characteristics of vibrating screen. The parallel axis space vibration model of the motors in three-dimensional space is proposed in the paper. In order to study the synchronous mechanism, the dynamic equations of the system are obtained according to the Lagrange formula. At the same time, the synchronization condition of the system is calculated by the mean small parameter method. Then, the synchronization stability of the system is studied by using Poincare - Lyapurov method. Finally, the correctness of the theoretical calculation is verified by numerical calculation. It is found that the system parameter values must satisfy both the synchronization conditions and the synchronization stability conditions to realize the stable synchronous operation between rotors. The synchronous state is determined by damping ratio, frequency ratio and motor position parameters. When the system operates in stable state, the motion trajectory of the vibrating screen's center of mass is an ellipse in the three-dimensional coordinate system.

Keywords

Vibration System; Synchronous; Vibrating Screen; Space Vibration.

1. Introduction

Synchronous phenomenon is ubiquitous in nature. In recent years, it has become one of the major scientific topics because of its important value and application prospect in engineering technologies such as nonlinear coupling system, complex network transmission system, coupling pendulum system and vibrating screen system [1-4]. The earliest synchronization phenomenon was discovered by Huygens in 1665 by observing the movement of two pendulums hanging on an elastic beam. The discovery and application of the theory stimulated the enthusiasm of scholars around the world in the study of synchronization theory and made many scientific research achievements. Blekhman (1988) discovered the synchronization of double excited motor in non-resonant system, and proposed the synchronization theory of double excited motor system by using Poincare Lyapunov method, which guides the application of synchronization theory in theoretical research and practical engineering [5]. In 2013, Czolczynski et al. considered the synchronization problem of the pendulum mounted on the horizontal beam, and derived the synchronization conditions of the system through analytical methods and numerical calculations [6]. In 2006, Hou Yongjun established a simulation model to consider the electromechanical coupling mechanism of three identical shaker systems, which is of great significance for discussing the synchronization problem of multi-motor driven vibration systems [7]. In 2009, Wen Bangchun et al. derived synchronization conditions and synchronization stability by using Hamilton theory and average method. The core idea of this method is to seek the equilibrium

ISSN: 2414-1895 DOI: 10.6919/ICJE.202105_7(5).0002

torque equation between motor shafts under synchronous state [8]. In 2010, Zhao Chunyu et al. studied an improved small-parameter method to state the synchronization process of motor system, which greatly simplified the solution process of system synchronization problem [9.10]. Zhang Xueliang et al. discussed the transmission mechanism of synchronous torque between cylindrical rollers and multi-rotors in the vibration system and revealed that in the synchronous state, the larger the maximum synchronous torque, the larger the allowable residual torque between motors [11.12.13]. In 2013-2014, Nanha Djanan et al. studied the system in which three motors work on the same board, and the synchronous operation of the rotor depends on the physical characteristics of the motor and the board [14,15]. Fang Pan et al. considered the synchronization and stability of the elastically coupled rotor in the vibration system and found that the synchronization characteristics of the system were affected by the stiffness of the coupled spring [16.17.18]. In 2016, Kong Xiangxi et al. realized the zero-phase synchronization state between the three rotors by using the adaptive synovial membrane control algorithm [19]. The above research mainly studies the synchronization of mechanical system in two - dimensional plane. Paz Cole (1992) and Chunyu Zhao (2010) discussed the spatial synchronization problem of two vertically unbalanced rotors [20.21]. In 2016, Chen Xiaozhe et al. carried out theoretical and experimental description on the spatial synchronization problem of unbalance rotors with the same rotating axis [22]. These studies explain the common vibration synchronization problems in daily life and promote the development of screening technology.

In this paper, a dynamic model of a space vibrating screen with non-parallel shafts motor for solid-liquid separation in drilling operations is studied. Motors synchronization have a decisive effect on the dynamic characteristics of vibration screen. Therefore, the study of motor synchronous state is the key to design of vibrating screen.

2. Dynamic model

A stucture diagram of the vibrating screen is shown in Figure 1(a). This vibrating screen includes a rigid vibrating body of mass m_4, which is elastically linked via damping springs with stiffness coefficient k_i and damping coefficient $f_i (i = x, y, z, \psi, \delta, \vartheta)$. Unbalanced rotor j is modeled by an eccentric structure $m_j (j = 1,2,3)$. The distance is r; The phase of the unblance rotor to the motor spin axis is $\varphi_j (j = 1,2,3)$. β is an intersection angle between $O_j G$ and Gx'; θ is an intersection angle between $z'''G$ and $z'G$; l is length between shaft center of the rotor to centroid G of the vibration body. The vibration system is oscillated in $x-, y-$ and $z-$directions, defined by displacements x, y and z. The body swung with respect to its centroid in $\psi-, \delta-$ and $\vartheta-$ directions, defined by displacements ψ, δ and ϑ.

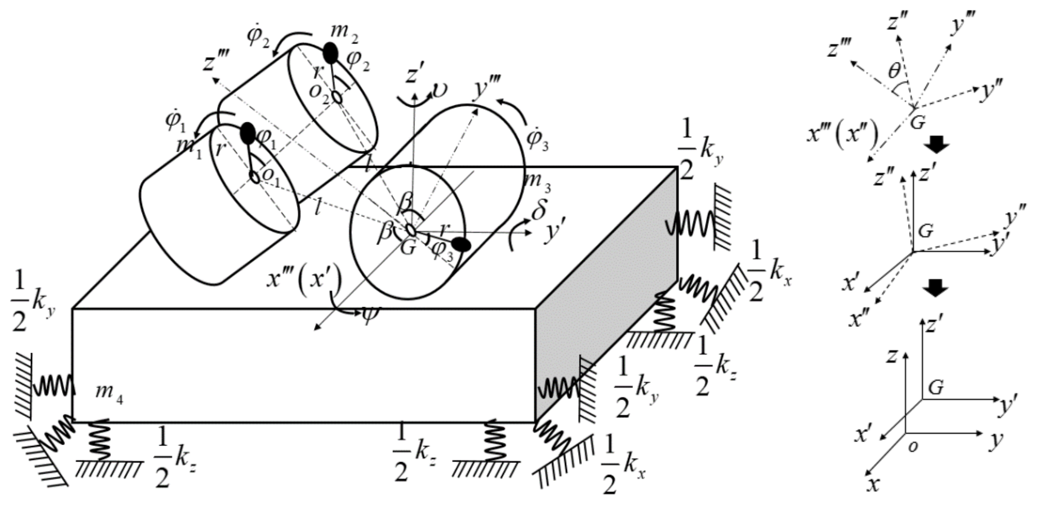

(a) dynamicmodel (b) reference coordinate

Figure 1. Dynamic model of the vibration screen

ISSN: 2414-1895 DOI: 10.6919/ICJE.202105_7(5).0002

The conversion of reference coordinate is shown in Figure 1(b), and spin order of the coordinate is abide by $Gx'''y'''z''' \rightarrow Gx''y''z'' \rightarrow Gx'y'z'$. The direction cosine matrix agreement with each coordinate spin can be denote by

$$A_1 = \begin{bmatrix} 1 & 0 & 0 \\ 0 & -\cos\theta & \sin\theta \\ 0 & \sin\theta & -\cos\theta \end{bmatrix}, A_2 = \begin{bmatrix} 1 & 0 & 0 \\ 0 & \cos\psi & -\sin\psi \\ 0 & \sin\psi & \cos\psi \end{bmatrix},$$
$$A_3 = \begin{bmatrix} \cos\delta & 0 & \sin\delta \\ 0 & 1 & 0 \\ -\sin\delta & 0 & \cos\delta \end{bmatrix}, A_4 = \begin{bmatrix} \cos\vartheta & -\sin\vartheta & 0 \\ \sin\vartheta & \cos\vartheta & 0 \\ 0 & 0 & 1 \end{bmatrix} \tag{1}$$

In consideration of infinitesimal rotation of the vibrating system in $\psi-, \delta-$and $\vartheta-$directions, matrices A_2, A_3 and A_4 are simplified as

$$A_2 = \begin{bmatrix} 1 & 0 & 0 \\ 0 & 1 & -\psi \\ 0 & \psi & 1 \end{bmatrix}, A_3 = \begin{bmatrix} 1 & 0 & \delta \\ 0 & 1 & 0 \\ -\delta & 0 & 1 \end{bmatrix}, A_4 = \begin{bmatrix} 1 & -\vartheta & 0 \\ \vartheta & 1 & 0 \\ 0 & 0 & 1 \end{bmatrix} \tag{2}$$

In spining coordinate $Gx'''y'''z'''$, center of mass coordinate of unbalanced rotor 1,2 and rotor 3 is expressed by

$$\boldsymbol{x}'''_1 = \begin{bmatrix} l\cos\beta - r\cos\varphi_1 \\ 0 \\ l\sin\beta + r\sin\varphi_1 \end{bmatrix}, \ \boldsymbol{x}'''_2 = \begin{bmatrix} -l\cos\beta - r\cos\varphi_2 \\ 0 \\ l\sin\beta + r\sin\varphi_2 \end{bmatrix}, \ \boldsymbol{x}'''_3 = \begin{bmatrix} 0 \\ r\sin\varphi_3 \\ r\cos\varphi_3 \end{bmatrix} \tag{3}$$

Center of mass coordinate of the eccentric lump in coordinate $Gx'y'z'$ can be acquired by means of the comvertion of spin matrix $\boldsymbol{R}$. Centroid of the oscillating screen in coordinate $oxyz$ is $\boldsymbol{x_G} = [x, y, z]^T$, and so center of mass of the rotors in coordinate $oxyz$ can be denoted by

$$\begin{cases} \boldsymbol{x}_1 = \boldsymbol{x_G} + A_1\boldsymbol{R}\boldsymbol{x}'''_1 \\ \boldsymbol{x}_2 = \boldsymbol{x_G} + A_1\boldsymbol{R}\boldsymbol{x}'''_2 \\ \boldsymbol{x}_3 = \boldsymbol{x_G} + A_1\boldsymbol{R}\boldsymbol{x}'''_3 \end{cases} \tag{4}$$

Where $\boldsymbol{R} = A_2A_3A_4$.

On the basis of kinetic theory, kinetic energy T, potential energy U and dissipated energy of the vibration body should be written by

$$\begin{aligned} E &= \frac{1}{2}m_4\left(\dot{x}^2+\dot{y}^2+\dot{z}^2\right)+\frac{1}{2}J_\psi\dot{\psi}^2+\frac{1}{2}J_\delta\dot{\delta}^2+\frac{1}{2}J_\vartheta\dot{\vartheta}^2 \\ &\quad+\frac{1}{2}\sum_{i=1}^{3}J_i\dot{\varphi}_i^2+\frac{1}{2}\sum_{i=1}^{3}m_i\dot{\mathbf{x}}_i^T\dot{\mathbf{x}}_i \\ U &= \frac{1}{2}k_xx^2+\frac{1}{2}k_yy^2+\frac{1}{2}k_zz^2+\frac{1}{2}k_\psi\psi^2+\frac{1}{2}k_\delta\delta^2+\frac{1}{2}k_\vartheta\vartheta^2 \\ D &= \frac{1}{2}f_x\dot{x}^2+\frac{1}{2}f_y\dot{y}^2+\frac{1}{2}f_z\dot{z}^2+\frac{1}{2}f_\psi\dot{\psi}^2+\frac{1}{2}f_\delta\dot{\delta}^2+\frac{1}{2}f_\vartheta\dot{\vartheta}^2 \\ &\quad+\frac{1}{2}f_1\dot{\varphi}_1^2+\frac{1}{2}f_2\dot{\varphi}_2^2+\frac{1}{2}f_3\dot{\varphi}_3^2 \end{aligned} \tag{5}$$

The dynamic equation of the vibration body above can be figured up. In the system, bring in $q_i = [x, y, z, \psi, \delta, \vartheta, \varphi_1, \varphi_2, \varphi_3]^T$ as generalized coordinate matrix, in addition, the generalized force matrix of the vibrating body is thought as $Q_i = [0,0,0,0,0,0, M_{e1} - R_{e\,1}, M_{e2} - R_{e\,2}, M_{e3} - R_{e\,3}\ ]^T$. the dynamic equations of the vibrating screen are written by

$$
\begin{aligned}
&M\ddot{x}+f_x\dot{x}+k_x x=-m_1 r\left(\ddot{\varphi}_1\sin\varphi_1+\dot{\varphi}_1^2\cos\varphi_1\right)-m_2 r\left(\ddot{\varphi}_2\sin\varphi_2+\dot{\varphi}_2^2\cos\varphi_2\right)\\
&M\ddot{y}+f_y\dot{y}+k_y y=m_1 r\sin\theta\left(\dot{\varphi}_1^2\sin\varphi_1-\ddot{\varphi}_1\cos\varphi_1\right)+m_2 r\sin\theta\left(\dot{\varphi}_2^2\sin\varphi_2-\ddot{\varphi}_2\cos\varphi_2\right)\\
&\qquad+m_3 r\left(\ddot{\varphi}_3\cos\theta\cos\varphi_3-\dot{\varphi}_3^2\cos\theta\sin\varphi_3+\ddot{\varphi}_3\sin\theta\sin\varphi_3+\lambda\dot{\varphi}_3^2\sin\theta\cos\varphi_3\right)\\
&M\ddot{z}+f_z\dot{z}+k_z z=m_1 r\cos\theta\left(\ddot{\varphi}_1\cos\varphi_1-\dot{\varphi}_1^2\sin\varphi_1\right)+m_2 r\cos\theta\left(\ddot{\varphi}_2\cos\varphi_2-\dot{\varphi}_2^2\sin\varphi_2\right)\\
&\qquad+m_3 r\left(-\ddot{\varphi}_3\sin\theta\cos\varphi_3+\dot{\varphi}_3^2\sin\theta\sin\varphi_3-\ddot{\varphi}_3\cos\theta\sin\varphi_3-\dot{\varphi}_3^2\cos\theta\cos\varphi_3\right)\\
&J_\psi\ddot{\psi}+f_\psi\dot{\psi}+k_\psi\psi=m_1 rl\sin2\theta\sin\beta\left(-\ddot{\varphi}_1\cos\varphi_1+\dot{\varphi}_1^2\sin\varphi_1\right)\\
&\qquad+m_2 rl\sin2\theta\sin\beta\left(-\ddot{\varphi}_2\cos\varphi_2+\dot{\varphi}_2^2\sin\varphi_2\right)\\
&J_\delta\ddot{\delta}+f_\delta\dot{\delta}+k_\delta\delta=m_1 rl\sin\beta\left(-\ddot{\varphi}_1\sin\varphi_1-\dot{\varphi}_1^2\cos\varphi_1\right)+m_1 rl\cos\beta\left(\ddot{\varphi}_1\cos\varphi_1-\dot{\varphi}_1^2\sin\varphi_1\right)\\
&\qquad+m_2 rl\sin\beta\left(-\ddot{\varphi}_2\sin\varphi_2-\dot{\varphi}_2^2\cos\varphi_2\right)+m_2 rl\cos\beta\left(-\ddot{\varphi}_2\cos\varphi_2+\dot{\varphi}_2^2\sin\varphi_2\right)\\
&J_\vartheta\ddot{\vartheta}+f_\vartheta\dot{\vartheta}+k_\vartheta\vartheta=m_1 rl\sin2\theta\cos\beta\left(\ddot{\varphi}_1\cos\varphi_1-\dot{\varphi}_1^2\sin\varphi_1\right)\\
&\qquad+m_2 rl\sin2\theta\cos\beta\left(-\ddot{\varphi}_2\cos\varphi_2+\dot{\varphi}_2^2\sin\varphi_2\right)\\
&J_1\ddot{\varphi}_1+f_1\dot{\varphi}_1=M_{e1}-R_{e1}-m_1 r\sin\varphi_1\left(\ddot{x}+\ddot{\delta}l\sin\beta\right)\\
&\qquad+m_1 r\cos\varphi_1\left(\ddot{z}\cos\theta-\ddot{y}\sin\theta+l\ddot{\vartheta}\sin2\theta\cos\beta+l\ddot{\delta}\cos\beta-l\ddot{\psi}\sin2\theta\sin\beta\right)\\
&J_2\ddot{\varphi}_2+f_2\dot{\varphi}_2=M_{e2}-R_{e2}-m_2 r\sin\varphi_2\left(\ddot{x}+\ddot{\delta}l\sin\beta\right)\\
&\qquad+m_2 r\cos\varphi_2\left(\ddot{z}\cos\theta-\ddot{y}\sin\theta-l\ddot{\vartheta}\sin2\theta\cos\beta-l\ddot{\delta}\cos\beta-l\ddot{\psi}\sin2\theta\sin\beta\right)\\
&J_3\ddot{\varphi}_3+f_3\dot{\varphi}_3=M_{e3}-R_{e3}+m_3 r\ddot{y}\left(\cos\theta\cos\varphi_3+\sin\theta\sin\varphi_3\right)\\
&\qquad-m_3 r\ddot{z}\left(\sin\theta\cos\varphi_3+\cos\theta\sin\varphi_3\right)
\end{aligned}
\tag{6}
$$

Where $M=m_1+m_2+m_3+m_4$. J_ψ, J_δ and J_ϑ on behalf of the moment of inertia of vibration screen about $\psi-$, $\delta-$and $\vartheta-$axis respectively. Here, $J_\psi\approx J_\delta\approx J_\vartheta\approx Ml_e^2$, in which l_e are assigned as the equivalent eccentricity radius of the oscillating screen around x-, y-, and z-directions. J_j is the rotational inertia of eccentric lump j, which is the sums of the rotary inertia of motor axis and eccentric lump. Compared with $m_j r^2$, the rotary inertia of motor axis is so tiny that can be ignore, i.e., $J_j\approx m_j r^2 (j=1,2,3)$. M_j and R_j are electromagnetic and frictional torque of the motor j. The dot over variables represents differentiation with respect to time t.

3. Synchronism of Rotors

The average phase angle of the unbalance rotors is regarded as φ, and the phase difference between the two eccentric rotors is assigned by α, i.e.

$$\varphi=\frac{1}{3}(\varphi_1+\varphi_2+\varphi_3), \varphi_1-\varphi_2=2\alpha_1, \varphi_2-\varphi_3=2\alpha_2 \tag{7}$$

$$\varphi_1=\varphi+\frac{4}{3}\alpha_1+\frac{2}{3}\alpha_2; \varphi_2=\varphi-\frac{2}{3}\alpha_1+\frac{2}{3}\alpha_2; \varphi_3=\varphi-\frac{2}{3}\alpha_1-\frac{4}{3}\alpha_2 \tag{8}$$

This vibrating screen is oscillated in a period. Hence, the variation of mean angle speed of the unbalance rotors is varied periodically. In light of the single mean period of the vibration body to be T, therefore the mean value of phase angle φ over the single period T must be a constant, i.e.

$$\omega_{m0}=\frac{1}{2}\int_0^T\dot{\varphi}\,dt=\text{constant} \tag{9}$$

ISSN: 2414-1895 DOI: 10.6919/ICJE.202105_7(5).0002

Considering the mean method and small parameter method, the coefficients of momentary fluctuation of $\dot{\varphi}$ and $\dot{\alpha}$ about ω_{m0} are assumed to be ξ_0, ξ_1 and ξ_2, which are functions of time t, i.e.

$$\dot{\varphi} = (1+\xi_0)\omega_{m0}, \dot{\alpha}_1 = \xi_1\omega_{m0}, \dot{\alpha}_2 = \xi_2\omega_{m0} \tag{10}$$

In light of equations (7) to (10), diffferentiate equation (10) with respect to t. The phase angle, angular velocity, and angular acceleration of the unbalance rotors can be writed by

$$\begin{aligned}
\dot{\varphi}_1 &= \left(1+\xi_0+\frac{4}{3}\xi_1+\frac{2}{3}\xi_2\right)\omega_{m0} = (1+\varepsilon_1)\omega_{m0} \\
\dot{\varphi}_2 &= \left(1+\xi_0-\frac{2}{3}\xi_1+\frac{2}{3}\xi_2\right)\omega_{m0} = (1+\varepsilon_2)\omega_{m0} \\
\dot{\varphi}_3 &= \left(1+\xi_0-\frac{2}{3}\xi_1-\frac{4}{3}\xi_2\right)\omega_{m0} = (1+\varepsilon_3)\omega_{m0}
\end{aligned} \tag{11}$$

When the mean values of small parameters $\varepsilon_1, \varepsilon_2$ and ε_3 in single mean period T are equal to zero, i.e., so as to acquire the approximate solutions of displacement of the vibration screen, lead in the following parameters

$$\begin{aligned}
&\eta_1 = m_1/M,\ \eta_2 = m_2/M,\ \eta_3 = m_3/M,\ \omega_x = \sqrt{k_x/M},\ \omega_y = \sqrt{k_y/M},\\
&\omega_z = \sqrt{k_z/M},\ \omega_\psi = \sqrt{k_\psi/J_\psi},\ \omega_\delta = \sqrt{k_\delta/J_\delta},\ \omega_\vartheta = \sqrt{k_\vartheta/J_\vartheta},\\
&\zeta_x = f_x/2\sqrt{Mk_x},\ \zeta_y = f_y/2\sqrt{Mk_y},\ \zeta_z = f_z/2\sqrt{Mk_z},\\
&\zeta_\psi = f_\psi/2\sqrt{J_\psi k_\psi},\ \zeta_\delta = f_\delta/2\sqrt{J_\delta k_\delta},\ \zeta_\vartheta = f_\vartheta/2\sqrt{J_\vartheta k_\vartheta},\ r_l = l/l_e
\end{aligned} \tag{12}$$

Substituting equation (12) into equation (6), the first six formulas in equation (10) can be expressed as

$$\begin{aligned}
&M\ddot{x} + f_x\dot{x} + k_x x = -m_1 r\dot{\varphi}_1^2\cos\varphi_1 - m_2 r\dot{\varphi}_2^2\cos\varphi_2\\
&M\ddot{y} + f_y\dot{y} + k_y y = m_1 r\dot{\varphi}_1^2\sin\theta\sin\varphi_1 + m_2 r\dot{\varphi}_2^2\sin\theta\sin\varphi_2\\
&\qquad + m_3 r\left(-\dot{\varphi}_3^2\cos\theta\sin\varphi_3 + \lambda\dot{\varphi}_3^2\sin\theta\cos\varphi_3\right)\\
&M\ddot{z} + f_z\dot{z} + k_z z = -m_1 r\dot{\varphi}_1^2\cos\theta\sin\varphi_1 - m_2 r\dot{\varphi}_2^2\cos\theta\sin\varphi_2\\
&\qquad + m_3 r\left(\dot{\varphi}_3^2\sin\theta\sin\varphi_3 - \lambda\dot{\varphi}_3^2\cos\theta\cos\varphi_3\right)\\
&J_\psi\ddot{\psi} + f_\psi\dot{\psi} + k_\psi\psi = m_1 rl\dot{\varphi}_1^2\sin 2\theta\sin\beta\sin\varphi_1 + m_2 rl\dot{\varphi}_2^2\sin 2\theta\sin\beta\sin\varphi_2\\
&J_\delta\ddot{\delta} + f_\delta\dot{\delta} + k_\delta\delta = -m_1 rl\dot{\varphi}_1^2\sin\beta\cos\varphi_1 - m_1 rl\dot{\varphi}_1^2\cos\beta\sin\varphi_1\\
&\qquad - m_2 rl\dot{\varphi}_2^2\sin\beta\cos\varphi_2 + m_2 rl\dot{\varphi}_2^2\cos\beta\sin\varphi_2\\
&J_\vartheta\ddot{\vartheta} + f_\vartheta\dot{\vartheta} + k_\vartheta\vartheta = -m_1 rl\dot{\varphi}_1^2\sin 2\theta\cos\beta\sin\varphi_1 + m_2 rl\dot{\varphi}_2^2\sin 2\theta\cos\beta\sin\varphi_2
\end{aligned} \tag{13}$$

The natural frequency of the vibration screen is thought as four to five times than frequency of exterior excitations in a far-resonant system, and damping ratio $\zeta_i(i = x, y, z, \psi, \delta, \vartheta)$ of the springs is extremely small. The displacements of the vibration body can be denoted as

ISSN: 2414-1895
DOI: 10.6919/ICJE.202105_7(5).0002

$$
\begin{aligned}
& x=-r\mu_x\left[-\eta_1\cos\left(\varphi_1-\gamma_x\right)-\eta_2\cos\left(\varphi_2-\gamma_x\right)\right] \\
& y=-r\mu_y\sin\theta\left[\eta_1\sin\left(\varphi_1-\gamma_y\right)+\eta_2\sin\left(\varphi_2-\gamma_y\right)\right] \\
& \quad -r\eta_3\mu_y\left[-\cos\theta\sin\left(\varphi_3-\gamma_y\right)+\lambda\sin\theta\cos\left(\varphi_3-\gamma_y\right)\right] \\
& z=-r\mu_z\cos\theta\left[-\eta_1\sin\left(\varphi_1-\gamma_z\right)-\eta_2\sin\left(\varphi_2-\gamma_z\right)\right] \\
& \quad -r\eta_3\mu_z\left[+\sin\theta\sin\left(\varphi_3-\gamma_z\right)-\lambda\cos\theta\cos\left(\varphi_3-\gamma_z\right)\right] \\
& \psi=-\mu_\psi\frac{rr_l\sin 2\theta\sin\beta}{l_e}\left[\eta_1\sin\left(\varphi_1-\gamma_\psi\right)+\eta_2\sin\left(\varphi_2-\gamma_\psi\right)\right] \\
& \delta=-\mu_\delta\frac{rr_l}{l_e}\left[-\eta_1\sin\left(\varphi_1-\gamma_\delta+\beta\right)+\eta_2\sin\left(\varphi_2-\gamma_\delta-\beta\right)\right] \\
& \vartheta=-\mu_\vartheta\frac{rr_l\sin 2\theta\cos\beta}{l_e}\left[-\eta_1\sin\left(\varphi_1-\gamma_\vartheta\right)+\eta_2\sin\left(\varphi_2-\gamma_\vartheta\right)\right]
\end{aligned}
\tag{14}
$$

Where $\mu_i = 1/\sqrt{(1-n_b^2)^2+(2\xi_i n_i)^2}$, $\gamma_i = arctan\frac{2\xi_i\omega_i/\omega_{m0}}{1-(\omega_i/\omega_{m0})^2}$.

4. Sychronous Condition

In light of equation (14), the second-order derivative of displacements in $x-, y-, z-, \psi-, \delta-$ and $\vartheta-$ directions with respect to t can be figured up. Leading up them into the last three formulas of equation (6), and integrating them over a period T. The equilibrium dynamics equation of the three motors is as follows:

$$
\begin{aligned}
J_1\dot{\bar{\varepsilon}}_1\omega_{m0} &= \bar{M}_{e1}-\bar{R}_{e1}-\frac{1}{2}Mr^2\omega_{m0}M_{L1}=P_1 \\
J_2\dot{\bar{\varepsilon}}_2\omega_{m0} &= \bar{M}_{e2}-\bar{R}_{e2}-\frac{1}{2}Mr^2\omega_{m0}M_{L2}=P_2 \\
J_3\dot{\bar{\varepsilon}}_3\omega_{m0} &= \bar{M}_{e3}-\bar{R}_{e3}-\frac{1}{2}Mr^2\omega_{m0}M_{L3}=P_3
\end{aligned}
\tag{15}
$$

The output electromagnetic torque of the motor can be denoted as:

$$M_{ej} = M_{eoj} - \bar{k}_{eoj}\bar{\varepsilon}_j, j = 1,2,3 \tag{16}$$

Where T_{e0j} and $\bar{k}_{eoj}$ represent the electromagnetic torque and angular velocity stiffness coefficients of the motor in the synchronous stable state. Substitute Equations (16) into Equation (15), and write the result in matrix form, i.e.

$$\boldsymbol{E}\dot{\bar{\varepsilon}} = \boldsymbol{G}\bar{\varepsilon} + \boldsymbol{U} \tag{17}$$

where

$$\dot{\bar{\boldsymbol{\varepsilon}}} = [\dot{\bar{\varepsilon}}_1 \quad \dot{\bar{\varepsilon}}_1 \quad \dot{\bar{\varepsilon}}_1]^T, \bar{\boldsymbol{\varepsilon}} = [\bar{\varepsilon}_1 \quad \bar{\varepsilon}_1 \quad \bar{\varepsilon}_1]^T, \boldsymbol{U} = [u_1 \quad u_2 \quad u_3]^T \tag{18}$$

$$\mathbf{E} = \begin{bmatrix} J_1\omega_{m0}+\chi'_{11} & \chi'_{12} & \chi'_{13} \\ \chi'_{21} & J_2\omega_{m0}+\chi'_{22} & \chi'_{23} \\ \chi'_{31} & \chi_{32} & J_3\omega_{m0}+\chi'_{33} \end{bmatrix};$$

$$\mathbf{G} = -\begin{bmatrix} k_{e01}+\chi_{11} & \chi_{12} & \chi_{13} \\ \chi_{21} & k_{e02}+\chi_{22} & \chi_{23} \\ \chi_{31} & \chi_{32} & k_{e03}+\chi_{33} \end{bmatrix}, \mathbf{U} = \begin{bmatrix} M_{e01}-R_{e01}-a_1 \\ M_{e01}-R_{e01}-a_1 \\ M_{e01}-R_{e01}-a_1 \end{bmatrix} \tag{19}$$

In the above equation, $\boldsymbol{E}$ represents the inertial coupling matrix between rotors; $\boldsymbol{G}$ and $\boldsymbol{U}$ represent the stiffness coupling matrix and load torque matrix. When the system are synchronous, the small parameter vectors $\dot{\bar{\boldsymbol{\varepsilon}}}$ and $\bar{\boldsymbol{\varepsilon}}$ must be zero. The equilibrium torque equation of the three motors can be obtained as follow.

ISSN: 2414-1895 DOI: 10.6919/ICJE.202105_7(5).0002

$$\begin{aligned}
M_{01}&=\bar{M}_{e01}-\bar{R}_{e1}=M_k\begin{Bmatrix}\omega_{m0}\eta_1^2W_{s01}+\omega_{m0}\eta_1\eta_2\left[W_{c1}\sin\left(2\bar{\alpha}_1+\theta_{c1}\right)+W_{s1}\cos\left(2\bar{\alpha}_1+\theta_{s1}\right)\right]\\+\omega_{m0}\eta_1\eta_3\left[W_{c3}\sin\left(2\bar{\alpha}_1+2\bar{\alpha}_2+\theta_{c3}\right)-W_{s3}\cos\left(2\bar{\alpha}_1+2\bar{\alpha}_2+\theta_{s3}\right)\right]\end{Bmatrix}\\
M_{02}&=\bar{M}_{e02}-\bar{R}_{e2}=M_k\begin{Bmatrix}\omega_{m0}\eta_1\eta_2\left[W_{c1}\sin\left(2\bar{\alpha}_1+\theta_{c1}\right)+W_{s1}\cos\left(2\bar{\alpha}_1+\theta_{s1}\right)\right]+\omega_{m0}\eta_2^2W_{s01}\\+\omega_{m0}\eta_2\eta_3\left[W_{c3}\sin\left(2\bar{\alpha}_2+\theta_{c3}\right)+W_{s3}\cos\left(2\bar{\alpha}_2+\theta_{s3}\right)\right]\end{Bmatrix}\\
M_{03}&=\bar{M}_{e03}-\bar{R}_{e3}=M_k\begin{Bmatrix}\omega_{m0}\eta_1\eta_3\left[W_{c3}\sin\left(2\bar{\alpha}_1+2\bar{\alpha}_2+\theta_{c3}\right)+W_{s3}\cos\left(2\bar{\alpha}_1+2\bar{\alpha}_2+\theta_{s3}\right)\right]\\+\omega_{m0}\eta_2\eta_3\left[W_{c3}\sin\left(2\bar{\alpha}_2+\theta_{c3}\right)+W_{s3}\cos\left(2\bar{\alpha}_2+\theta_{s3}\right)\right]+\omega_{m0}\eta_3^2W_{s03}\end{Bmatrix}
\end{aligned}\tag{21}$$

where M_{0j} represents the output torque in motor j, which is the difference between the electromagnetic torque of the motors and fractional toques in their axis. $M_k=Mr^2\omega_{m0}^2/2$ represents the kinetic of the system. Since the sine value of the phase lag angle is much smaller than the cosine value, the coefficients W_{s1} and W_{s3} can be ignored. Considering equation (20), we have

$$\frac{\Delta M_{012}}{M_k}-\eta_2^2W_{s01}-\eta_2^2W_{s01}=\tau_{12}(2\bar{\alpha}_1,2\bar{\alpha}_2);\frac{\Delta M_{023}}{M_k}-\eta_2^2W_{s01}+\eta_3^2W_{s03}=\tau_{23}(2\bar{\alpha}_1,2\bar{\alpha}_2)\tag{21}$$

where

$$\begin{aligned}
\tau_{12}\left(2\bar{\alpha}_1,2\bar{\alpha}_2\right)&=2\eta_1\eta_2\left[W_{c1}\sin\left(2\bar{\alpha}_1+\theta_{c1}\right)\right]\\
&\quad+\eta_1\eta_3\left[-W_{c3}\cos\left(2\bar{\alpha}_1+2\bar{\alpha}_2+\theta_{c3}\right)+W_{s3}\sin\left(2\bar{\alpha}_1+2\bar{\alpha}_2+\theta_{s3}\right)\right]\\
&\quad-\eta_2\eta_3\left[-W_{c3}\cos\left(2\bar{\alpha}_2+\theta_{c3}\right)+W_{s3}\sin\left(2\bar{\alpha}_2+\theta_{s3}\right)\right]\\
\tau_{23}\left(2\bar{\alpha}_1,2\bar{\alpha}_2\right)&=\eta_1\eta_2\left[-W_{c1}\sin\left(2\bar{\alpha}_1+\theta_{c1}\right)+W_{s1}\cos\left(2\bar{\alpha}_1+\theta_{s1}\right)\right]\\
&\quad+2\eta_2\eta_3\left[-W_{c3}\cos\left(2\bar{\alpha}_2+\theta_{c3}\right)\right]\\
&\quad-\eta_1\eta_3\left[W_{c3}\cos\left(2\bar{\alpha}_1+2\bar{\alpha}_2+\theta_{c3}\right)+W_{s3}\sin\left(2\bar{\alpha}_1+2\bar{\alpha}_2+\theta_{s3}\right)\right]
\end{aligned}\tag{23}$$

In Equation (21), the left side of the equal represents the difference of the residual torques of the two motors, and the right side of the equal represents the dimensionless coupling torques between the two motors. $\tau_{c12}(2\bar{\alpha}_1,2\bar{\alpha}_2)$ is abounded function with respect to α_1 and α_2.i.e.,

$$\left|\frac{\Delta M_{012}}{M_k}-\eta_2^2W_{s01}-\eta_2^2W_{s01}\right|=|\tau_{12}(2\bar{\alpha}_1,2\bar{\alpha}_2)|\left|\frac{\Delta M_{023}}{M_k}-\eta_2^2W_{s01}+\eta_3^2W_{s03}\right|=|\tau_{23}(2\bar{\alpha}_1,2\bar{\alpha}_2)|\tag{23}$$

$$|\tau_{12}(2\bar{\alpha}_1,2\bar{\alpha}_2)|\le\tau_{12\,max}\ (2\bar{\alpha}_1,2\bar{\alpha}_2);\ |\tau_{23}(2\bar{\alpha}_1,2\bar{\alpha}_2)|\le\tau_{23\,max}\ (2\bar{\alpha}_1,2\bar{\alpha}_2)\tag{24}$$

Thus, to guarantee that the exciters are synchronously rotated, the synchronous condition of the vibration body can be described that maximum value of the non-dimensional coupling torque between the two motors should be bigger than or identical with difference of the dimensionless surplus torque. Finally, assumption the balanced torque to be P_j. On the basis of Poincare-Lyapunov method, equilibrium torque equation of the motor is applied to search the synchronous stability condition of the vibrating system. i.e.,

$$\begin{vmatrix}\frac{\partial(P_1-P_2)}{\partial 2\alpha_1}-\chi & \frac{\partial(P_1-P_2)}{\partial 2\alpha_2}\\ \frac{\partial(P_2-P_3)}{\partial 2\alpha_1} & \frac{\partial(P_2-P_3)}{\partial 2\alpha_2}-\chi\end{vmatrix}=0\tag{25}$$

In light of Poincare-Lyapunov method, to insure that the system exists stable approximation solutions, the real part of each solution χ in Eq. (25) should be minus. Therefore, through Eq. (25), two roots χ_1 and χ_2 relevant to steady phase differences can be calculated as follows:

$$\chi_1=\frac{a+d+\sqrt{(a+d)^2-4(ad-bc)}}{2}<0,\chi_2=\frac{a+d-\sqrt{(a+d)^2-4(ad-bc)}}{2}<0\tag{26}$$

ISSN: 2414-1895 DOI: 10.6919/ICJE.202105_7(5).0002

5. Numerical Anlysis

The essence of autosynchronization of the three motor excitation in spacial has been discribed by the above-mentioned theory in detail. In order to further comprehension the theory of synchronization stability among the tri-exciters, it is essential to perform some arithmetic computations. Hence, the basic parameters of the system are considered as follows: $k_{\psi} = 13560(\text{N/m})$, $k_x = k_y = k_z = 89586(\text{N/m})$ $f_x = f_y = f_z = 207(N \cdot \text{s/m})$, $f_{\psi} = 150(N \cdot \text{s/rad})$, $m_4 = 100(\text{kg})$, $r = 0.1(m)$, $J_m = 10(\text{kgm}^2)$, $\omega_{m0} = 157(\text{rad/s})$.

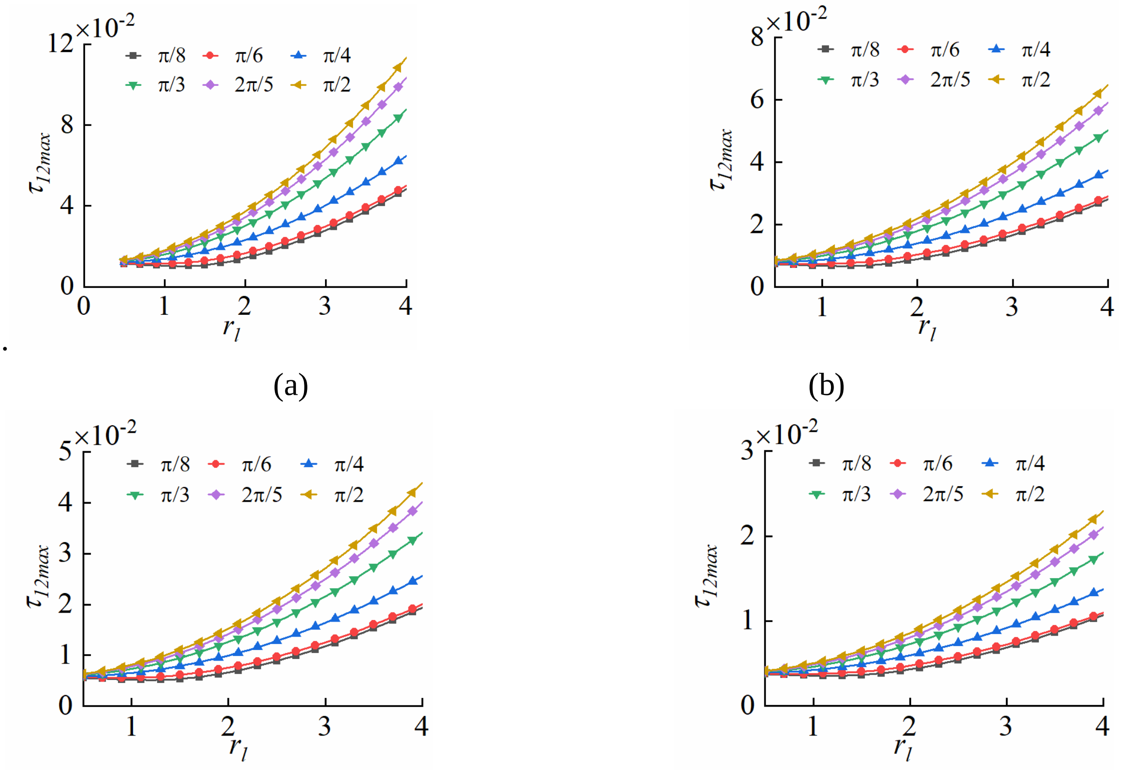

(c) (d)

Figure 2. The value of the dimentionless coupling torque: (a) $\eta_1 = \eta_2 = \eta_3 = 0.04$, (b) $\eta_1 = \eta_2 = 0.03$, $\eta_3 = 0.04$, (c) $\eta_1 = 0.02$, $\eta_2 = 0.03$, $\eta_3 = 0.04$, (d) $\eta_1 = 0.01$, $\eta_2 = 0.03$, $\eta_3 = 0.04$

The variating trend of the maximum value of the dimensionless coupling torque with r_l is discussed as shown in Figure 2. The mass ratio is equal in (a), and the mass ratio is not equal in (b) ~ (d). The dimensionless coupling torque increases when r_l increases. When r_l is constant, $\tau_{12\,max}$ also increases with the increase of β, and the larger β is, the faster the value of b increases. When the mass ratio is both 0.04, the value of a is the largest. Under this condition, the difference of remanent torque between the two motors allowed for synchronous operation of the vibration screen is the largest.

6. Computer Simulation

Some computer simulation can be obtained according to the dynamics equation (6). The values of the parameters in the simulation are as follows: rated power 0.07 Kw, rated voltage 220 v, frequency 50 Hz, the rotating speed of 157 rad/s, stator resistance 0.56 Ω and rotor resistance 0.54 Ω, stator inductance 0.1 H, rotor inductance 0.12 H, the mutual inductance 0.13H, the damping coefficient of motor shaft 0.01 N/m, $k_x \approx k_y \approx k_z = 98596, k_{\psi} \approx k_{\delta} \approx k_{\vartheta} = 19719$, $l = 0.5$, $f_x \approx f_y \approx f_z = 207$, $r = 0.05$, $f_{\psi} \approx f_{\delta} \approx f_{\vartheta} = 150$, $\theta = \pi/4$, $\beta = \pi/6$. The electromechanical coupling model was built in Simulink, and the system dynamics characteristics were obtained as follows.

ISSN: 2414-1895 DOI: 10.6919/ICJE.202105_7(5).0002

When $\eta_1 = \eta_2 = \eta_3 = 0.04$, the dynamic characteristics of the screen are shown in Figure 3. The rotational speed of the three motors fluctuates around 157rad/s in Figure 3(a). The phase difference between 1 and 2 motor is stable at -1.5rad, which is in perfect keeping with the theoretical calculation. The motion track of the vibrating body center is an ellipse in space, and the projection on the zoy plane is a straight line. The motion trajectory of the vibration body is an ellipse in the spatial coordinate. The displacement of the centroid in the $x-, y-$and $z-$directions is shown in Figure 3(d)~(f). The vibration displacement of the screen in the $y-, z-$direction is slightly less than the displacement in the $z-$direction.

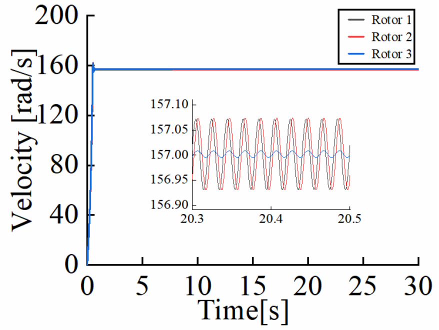

(a) Rotor velocity

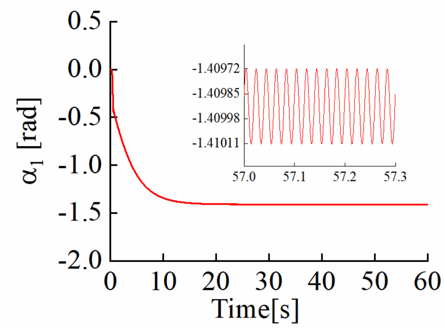

(b) phase difference

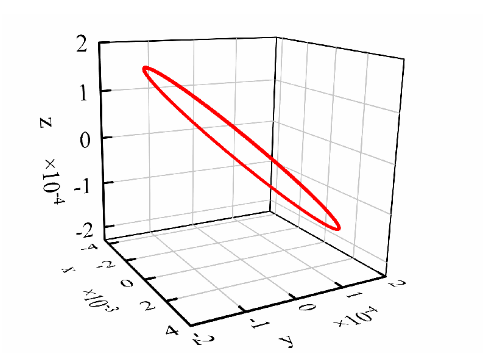

(c) trajectory of the system

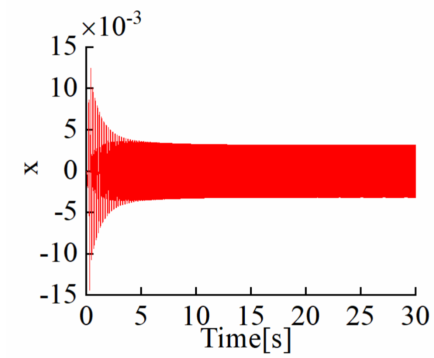

(d) displacement in x direction

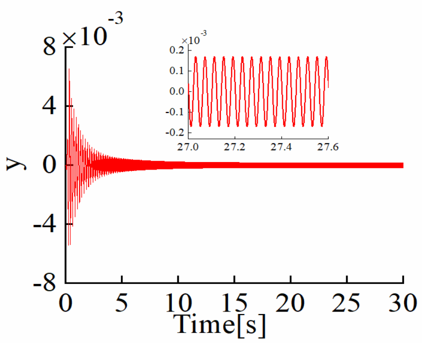

(e) displacement in y direction

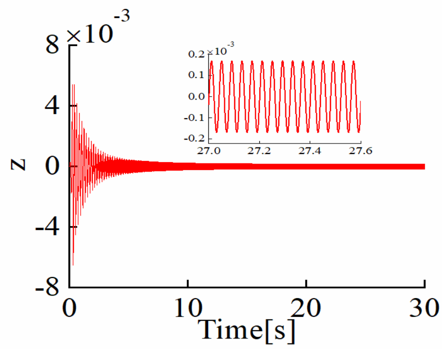

(f) displacement in z direction

Figure 3. Dynamic characteristics for $\eta_1 = \eta_2 = \eta_3 = 0.04$, $r_l = 1$.

7. Conclusion

In order to reduce the possibility of screen blocking, this paper presents a kind of non-parallel axis three-motor self-synchronous vibrating screen. The self-synchronization of the vibration screen is described in detail by using small parameter method and Poincare-Lyapunov theory. The results show that the maximum dimensionless coupling torque should be bigger than or equal to the difference of the dimensionless residual torque in order to insure the synchronous motion of the driver. In addition, based on the equation, the criterion of synchronization stability between rotors is derived, and when the two roots related to the phase difference are less than zero, the system has a stable approximate

ISSN: 2414-1895 DOI: 10.6919/ICJE.202105_7(5).0002

solution. When the parameters of the system meet both the synchronous condition and the synchronous stability condition, the auto-synchronization of the system can be realized. In this paper, the mechanism of synchronous stabilization is further discussed by numerical calculation and simulation. The results of the study found that the dimensionless coupling torque between motors increases with the increase of r_l, and the greater the β value is, the greater the dimensionless coupling torque is. When r_l is smaller, the system is easier to achieve synchronization. The phase difference in the stable phase is obviously affected by the motor installation position.

References

[1] Jiang, C.M., Zhang, F.F., Li, T.X.: Synchronization and anti-synchronization of N-coupled fractional-order complex chaotic systems with ring connection. Mathematical Methods in the Applied Sciences. 41(7), 2625-2638 (2018).

[2] Arenas, A., Díaz-Guilera, A., Kurths, J.,Moreno, Y., Zhou, C.S.: Synchronization in complex networks. Physics Reports. 469(3), 93-153 (2008).

[3] Warminski, J., Szmit, Z., Latalski, J.: Nonlinear dynamics and synchronization of pendula attached to a rotating hub. The European Physical Journal-Special Topics. 223(4), 827-847 (2014).

[4] Fang, P., Hou, Y.J.: Synchronization characteristics of a rotor-pendula system in multiple coupling resonant systems. Proceedings of the Institution of Mechanical Engineers. Part C: Journal of Mechanical Engineering Science. 232(10), 1802-1822 (2018).

[5] Blekhman I.I., 1988, Synchronization in Science and Technology, ASME Press, New York.

[6] Czolczynski K., 2013, Synchronization of the self-excited pendula suspended on the vertically displacing beam, Communications in Nonlinear Science and Numerical Simulation, 18, 2, 386-400.

[7] Hou, Y.J., Yan, G.X.: Electromechanical Dynamics Simulation of Complex Frequency Vibrating Screen with Two-Motor-Driving[J]. Applied Mechanics and Materials.2012,271-272:1211-1217.

[8] Wen B.C., Fan J., 2009, Synchronization and Controlled Synchronization in Engineering, Science Press, Beijing.

[9] Zhao C.Y., Zhang Y.M., 2010a, Synchronization and general dynamic symmetry of a vibrating system with two exciters rotating in opposite directions, Chinese Physics B, 19, 3.

[10] Zhao C.Y., Zhu H.T., 2010, Synchronization of two coupled exciters in a vibrating system of spatial motion, Acta Mechanica Sinica, 26, 477-493.

[11] Zhang X.L., Wen B.C., Vibratory synchronization transmission of two exciters in a super-resonant vibrating system, Journal of Mechanical Science and Technology, 28, 6,2049-2058.

[12] Zhang X.L., Wen B.C., 2016, Theoretical study on synchronization of two exciters in a nonlinear vibrating system with multiple resonant types, Nonlinear Dynamics, 85, 1, 141-154.

[13] Zhang X.L., Wen B.C., 2017, Vibratory synchronization transmission of a cylindrical roller in a vibrating mechanical system excited by two exciters, Mechanical Systems and Signal Processing, 96, 88-103.

[14] Nanha Djanan A.A., Woafo P., 2013, Electromechanical control of vibration on a plate submitted to a non-ideal excitation, Mechanics Research Communications,54, 72-82.

[15] Nanha Djanan A.A., Nana Nbendjo B.R., 2014, Effect of self-synchronization of DC motors on the amplitude of vibration of a rectangular plate, The European Physical Journal Special Topics, 223, 813-825.

[16] Fang P., Hou Y.J., 2018, Synchronization behavior of triple-rotor-pendula system in a dual –super-far resonance system, Proceedings of The Institution of Mechanical Engineers Part C Journal of Mechanical Engineering Science. (232):10, 1620-1640.

[17] Fang P., Yang Q.M., Hou Y.J., 2014, Theoretical study on self-synchronization of two homodromy rotors coupled with a pendulum rod in a far-resonant vibrating system, Journal of Vibroengineering, 16, 5, 2188-2204.

[18] Hou Y.J., Du M.J., Fang P., Zhang L., 2018, Synchronization and stability of an elastically coupled tri-rotor vibration system, Journal of Theoretical and Applied Mechanics, 55, 1, 227.